

Single-Shot Frequency-resolved Imbalance Characterization for Coherent Transceivers Based on Inter-channel Response Ratio

Honglin Ji^(1, 2), Jingchi Li⁽³⁾, Xingfeng Li⁽³⁾, Zhen Wang⁽³⁾, Ranjith Rajasekharan Unnithan⁽³⁾, Yikai Su⁽³⁾, Weisheng Hu^(1, 3), and William Shieh⁽²⁾

⁽¹⁾ Peng Cheng Laboratory, Shenzhen, China, jihl@pcl.ac.cn.

⁽²⁾ Department of Electrical and Electronic Engineering, The University of Melbourne, VIC 3010, Australia.

⁽³⁾ State Key Lab of Advanced Optical Communication Systems and Networks, Shanghai Jiao Tong University, Shanghai 200240, China.

Abstract We propose a simple but efficient method to simultaneously characterize the frequency-resolved IQ and polarization imbalance by a single-shot measurement for coherent transceivers based on the simple inter-channel response ratio. We demonstrate the characterization through a successful transmission of a 75-Gbaud PCS-256QAM signal with a 1.05-Tb/s raw data rate. ©2022 The Author(s)

Introduction

To further increase the speed of the short-reach optical communication systems, the coherent transmission technology is being introduced to realize the higher-order modulation formats and faster signaling rate [1], which makes the coherent systems more vulnerable to the hardware imperfections of both the transmitters and receivers. Generally, the imperfections of the coherent transceivers comprise the IQ and polarization imbalance. The IQ and polarization imbalances are referred to the amplitude and phase imbalance for each polarization and between two polarization tributaries, respectively. The IQ imbalance could result in the linear self-interference by the conjugate signal [2], which can severely hamper the coherent transmission performance as this imperfection could weaken the capability of the post DSP for channel impairments compensation. Although the polarization imbalance can be eventually compensated by the coherent detection, it would be good to be compensated before DSP.

However, the amplitude and phase imbalance are normally frequency-dependent. As part of the frequency-dependent phase imbalance, the constant IQ and polarization skews are normally estimated including using the reconfigurable interference [3], single sideband (SSB) signals [4], and digital pre-distortion scheme [5]. Also, as part of the frequency-dependent amplitude imbalance, the constant IQ amplitude imbalance has been evaluated by using machine learning [6]. To fully assess those imbalances, the signal-carrier interleaved direct detection receiver [7] and phase retrieval technique using one PD [8] are studied recently. However, they all have high implementation complexity. Therefore, it is quite challenging to estimate the frequency-resolved imbalance in a single shot test.

In this paper, we propose, for the first time, a

simple but efficient method to simultaneously characterize the frequency-resolved IQ and polarization amplitude and phase imbalance residing at either the transmitter or the receiver based on the single-shot measurement of the inter-channel response ratio. To estimate the transmitter-side imbalance, only one single-ended PD is required. To quantify the receiver-side imbalance, the measurement is based on the standard coherent receiver without modification. The effectiveness and performance of our proposed approaches are verified by the successful recovery of a 75-Gbaud dual-polarization (DP) PCS-256QAM signal with a 1.05-Tb/s raw data rate.

Principle of the proposed approach for estimating the frequency-resolved imbalance

The conceptual diagram of the proposed method for estimating the transmitter-side imbalance is presented in Fig. 1(a). Only one single-ended PD for direct detection is employed to characterize both the frequency-dependent IQ and polarization imbalance of the employed DP IQ modulator. Since the IQ modulator is normally biased at the null point, the EDFA is employed to boost the optical power. The optical output $E(t)$ from the DP IQ modulator can be given by

$$E(t) = s_1^x(t) + js_2^x(t - \tau_2) \otimes h_2(t) + s_3^y(t - \tau_3) \otimes h_3(t) + js_4^y(t - \tau_4) \otimes h_4 \quad (1)$$

where $s_i^{x/y}(t)$ ($i = 1, 2, 3, 4$) represent the four channels XI/XQ/YI/YQ as shown in Fig. 1(a); τ_i is the corresponding time skew referred to the s_1 channel; $h_i(t)$ describes the frequency-dependent imbalance referred to the s_1 channel; \otimes stands for the convolution operation. In Eq. (1), the IQ/polarization time skews are factored out from the frequency-dependent phase imbalance. Hence, the IQ skews of the two channels inside the DP IQ modulator are τ_2 and $\tau_4 - \tau_3$,

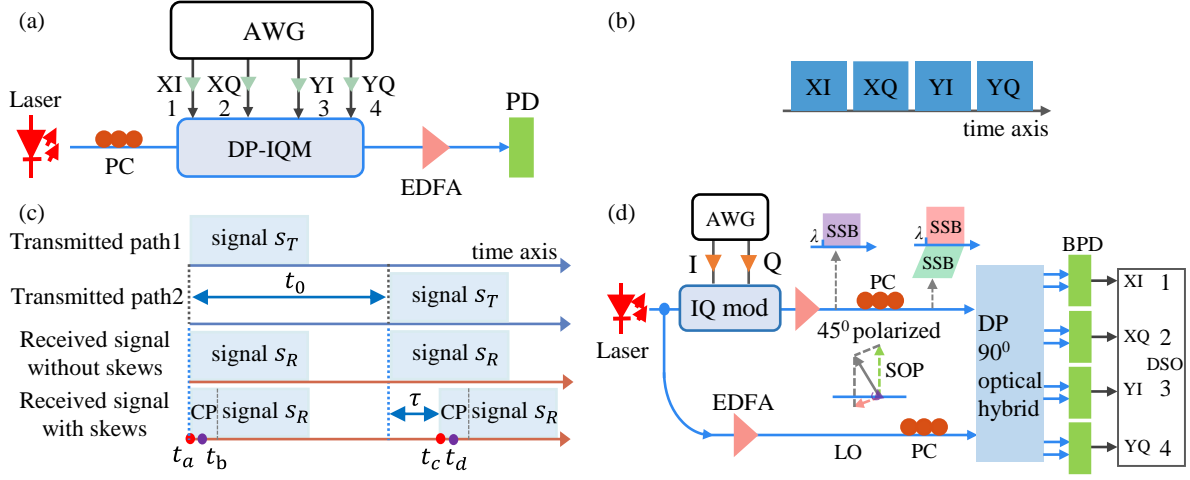


Fig. 1: (a) Experimental setup for estimating transmitter-side imbalance. (b) Time allocation of the probe signals for the four channels without overlap at the transmitter. (c) Schematic of time skew between two measured paths at the transmitter. (d) Experimental setup for estimating receiver-side imbalance. DP-IQM: dual-polarization IQ modulator. CP: cyclic prefix.

respectively. The polarization skew between the two polarization tributaries is τ_3 . The frequency-dependent IQ imbalance for the two polarizations is $h_2(t)$ and $h_4(t) \otimes h_3^{-1}(t)$. The frequency-dependent polarization imbalance between the two polarization tributaries is $h_3(t)$. To estimate these imperfections, the transmitted probe signal is expressed as

$$s_i(t) = c + s(t) \quad (i = 2,3,4) \quad (2)$$

where c is the constant optical carrier for channel linearization; $s(t)$ is the subcarrier-interleaved (i.e., odd-subcarrier-loaded) discrete multi-tone (DMT) signal to avoid the second-order distortion from the single-ended PD. To characterize these imperfections in a single-shot measurement, the four channels of the DP IQ modulator in Fig. 1 (b) are with the same probe signal but without the overlap in the time domain. Fig. 1(c) illustrates the two channels under test with/without time skew. Without the time skew, the time interval between the two channels is equal to the pre-set value t_0 . When the time skew τ ($\tau = t_{ac} - t_0$) exists, the time interval between the two probe signals is $t_0 + \tau$. To estimate the frequency-dependent imbalance including the time skew, the sample points t_b and t_d within the cyclic prefix are used for the two probe signals in practice instead of the ideal sample points t_a and t_c . This timing induced time mismatch is denoted as $\Delta\tau = t_{bd} - t_{ac}$. Then, the inter-channel response ratio between the two probe signals in the frequency domain can be obtained as

$$R_i(f) = \frac{F[s(t + \Delta\tau_i) \otimes h_i(t)]}{F[s(t)]} = H_i(f) e^{j2\pi f \Delta\tau_i} \quad (3)$$

where $F[\cdot]$ represents the *Fourier* transform and f is the used subcarrier frequency. To eliminate the timing induced error $\Delta\tau$, the linear regression for the phase response of $R_i(f)$ is performed to find out the slope k_i . The timing error $\Delta\tau_i$ and time skew τ_i can be obtained by

$$\Delta\tau_i = \frac{k_i}{2\pi} \quad (i = 2,3,4) \quad (4)$$

$$\tau_i = t_{ac} - t_0 = t_{bd} - \Delta\tau_i - t_0 \quad (5)$$

Eliminating the obtained $\Delta\tau_i$ for Eq. (3), the frequency-dependent imbalance $H_i(f)$ could be derived including the phase and amplitude imbalance.

Fig. 1(d) shows the experimental setup to estimate the receiver-side frequency-dependent imbalance. The probe signal used is an SSB-based OFDM signal. Before being fed into the coherent receiver, the SSB OFDM signal is oriented at approximately 45 degrees to the local receiver polarizations by using a polarization controller. The same laser source is used for the receiver to simplify the DSP. Since the received four channels are in parallel, namely no pre-set value t_0 , the time skews can be directly obtained by Eq. (4). The frequency-dependent imbalance for the receiver can be estimated by Eq. (3).

Results and discussion

To first prove the principle for transmitter characterization, the DMT-modulated signal is generated with 4096-point FFT, in which 768 odd-indexed subcarriers are utilized within 37.5-GHz bandwidth. The loaded signal for the DMT is the QPSK symbol. The constant carrier is added to the DMT for generating the probe signal for transmitter-side imbalance characterization. In this experiment, the carrier-signal power ratio (CSPR) is optimized to be 2 dB. The OSNR of the generated probe signal from the DP IQ modulator is 30 dB under test. Following the DSP described above, the frequency-dependent IQ/polarization amplitude and phase imbalance of $R_i(f)$ are obtained and shown in Fig. 2(a) and Fig. 2(b), respectively. By using the linear interpolation for the phase curves, the timing error could be obtained by Eq. (4) and the estimated time skew between XI and XQ, XI and YI, XI and YQ are

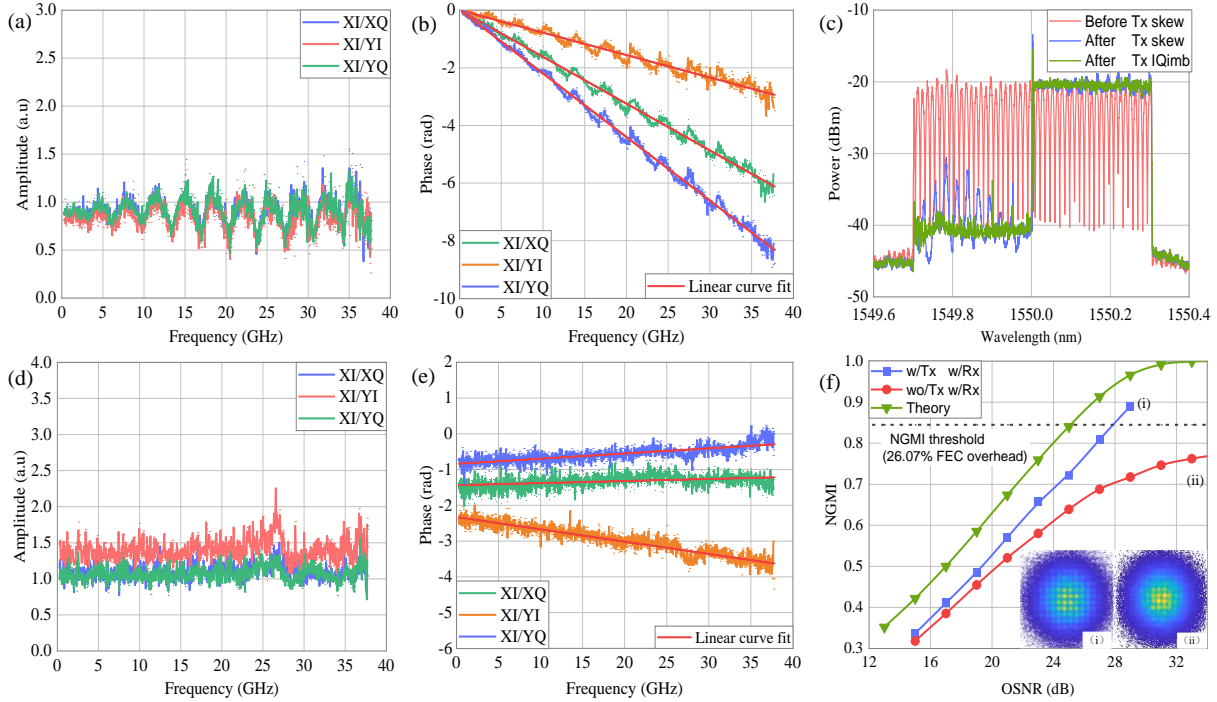


Fig. 2: Estimated transmitter-side frequency-dependent imbalance of (a) amplitude response and (b) phase response at the 2-dB CSPR and 30-dB OSNR. (c) Measured optical spectrum of an SSB signal with/without imbalance compensation. Estimated receiver-side frequency-dependent imbalance of (e) amplitude response and (f) phase response at the OSNR of 35 dB. (f) NGMI performance as a function of OSNR. w/wo/Tx/Rx: with/without transmitter/receiver-side all imbalance compensation.

645.87 ps, 622.37 ps, and 605.14 ps, respectively. Inferred from the estimated time skew, the two IQ skews (τ_2 and $\tau_4 - \tau_3$) and the polarization skew between (τ_3) are 645.87 ps, 17.23 ps, and 23.5 ps, respectively. The fluctuation on the phase curves in Fig. 2(b) signifies the frequency-dependent phase imbalance. To examine the effectiveness of the above results, the SSB signal with/without the IQ imbalance pre-compensation is presented in Fig. 2(c). Without the IQ skew compensation, the optical spectra of the SSB signal have significant leakage in the mirror image of the signal, which is generated by the linear self-interference [2]. With the IQ skew compensation, the image of the SSB is successfully suppressed. The ripples on the image spectrum imply the frequency-dependent amplitude imbalance, which is the same as our estimated results in Fig. 2(a) and demonstrates the effectiveness of our method. After the frequency-dependent imbalance compensation, the ripples are successfully suppressed.

To estimate the receiver-side imperfections, the used OFDM SSB signal possesses 1536 subcarriers within 37.5-GHz bandwidth. Following the similar DSP as the transmitter, the receiver-side frequency-dependent amplitude and phase imbalance are shown in Figs. 2(d), and 2(e), respectively. The slope of phase curves in Fig. 2(e) is determined by the receiver-side IQ and polarization skews. By using Eq. (4), The estimated time skew between XI and XQ, XI and

YI, and XI and YQ are 0.99 ps, 5.38 ps, and 2.32 ps, respectively. Therefore, the receiver-side polarization skew is 5.38 ps and the two IQ skew are 0.99 ps and 3.06 ps, respectively. Note that the skew estimation accuracy of the proposed method for both transceivers could be further improved by using a large number of subcarriers.

To confirm the effectiveness of our proposed method for transceiver calibration, a 1.05-Tb/s DP coherent transmission experiment using 7 bit/symbol PCS-256QAM is conducted, which is shown in Fig. 2(f). Without the receiver-side imbalance compensation, the complex-valued 2x2 MIMO could not converge. With the transmitter-side frequency-resolved imbalance compensation, the 1.05-Tb/s transmission is successfully achieved to reach the NGMI threshold. These experimental results signify the effectiveness and advantages of our proposed approaches for coherent transceiver calibration.

Conclusions

In this paper, we propose a simple but efficient approach to characterize both the transmitter- and receiver-side frequency-dependent IQ/polarization imbalance in a single-shot test. The transmitter-side calibration only employs one PD, and the receiver-side calibration is based on the standard coherent receiver. The effectiveness of our proposed method is confirmed by a 1.05-Tb/s transmission using a 75-Gbaud PCS-256QAM signal.

References

- [1] X. Zhou, R. Urata and H. Liu, "Beyond 1 Tb/s Intra-Data Center Interconnect Technology: IM-DD OR Coherent?," in *Journal of Lightwave Technology*, vol. 38, no. 2, pp. 475-484, 15 Jan.15, 2020.
- [2] E. P. Silva and D. Zibar, "Widely linear equalization for IQ imbalance and skew compensation in optical coherent receivers," *J. Lightw. Technol.*, vol. 34, no. 15, pp. 3577–3586, Aug. 2016.
- [3] Y. Yue, B. Zhang, Q. Wang, R. Lofland, J. O'Neil, and J. Anderson, "Detection and alignment of dual-polarization optical quadrature amplitude transmitter IQ and XY skews using reconfigurable interference," *Opt. Express* 24(6), 6719–6734 (2016).
- [4] H. Chen, X. Su, Z. Tao, T. Oyama, H. Nakashima, T. Hoshida, and K. Kato, "An accurate and robust inphase/quadrature skew measurement for coherent optical transmitter by image spectrum analyzing," in *Proc. Eur. Conf. Opt. Commun.*, 2017, pp. 1–3.
- [5] G. Khanna, B. Spinnler, S. Calabrò, E. de Man, Y. Chen, and N. Hanik., "Accurate estimation of transmitter I/Q skew for high-rate spectrally efficient optical transponders," in *Proc. Eur. Conf. Opt. Commun.*, Sep. 2018, pp. 1–3.
- [6] X. Dai, X. Li, M. Luo, and S. Yu, "Numerical simulation and experimental demonstration of accurate machine learning aided IQ time-skew and power-imbalance identification for coherent transmitters," *Opt. Express* 27, 38367-38381 (2019).
- [7] X. Chen and D. Che, "Direct-Detection Based Frequency-Resolved I/Q Imbalance Calibration for Coherent Optical Transmitters," in *Optical Fiber Communication Conference (OFC) 2021*, paper Th5D.3.
- [8] H. Chen, H. Huang, N. K. Fontaine, and R. Ryf, "Phase retrieval with fast convergence employing parallel alternative projections and phase reset for coherent communications," *Opt. Lett.* 45, 1188-1191 (2020).